

Shock Propagation in Granular Flow Subjected to an External Impact

Sudhir N. Pathak,^{1,*} Zahera Jabeen,^{2,†} Purusattam Ray,^{1,‡} and R. Rajesh^{1,§}

¹*Institute of Mathematical Sciences, CIT Campus, Taramani, Chennai-600113, India*

²*Department of Physics, University of Michigan, Ann Arbor, MI 48109-1040, USA*

(Dated: May 17, 2012)

We analyze a recent experiment [Phys. Rev. Lett., **103**, 224501 (2009)] in which the shock, created by the impact of a steel ball on a flowing monolayer of glass beads, is quantitatively studied. We argue that radial momentum is conserved in the process, and hence show that in two dimensions the shock radius increases in time t as a power law $t^{1/3}$. This is confirmed in event driven simulations of an inelastic hard sphere system. The experimental data are compared with the theoretical prediction, and is shown to compare well at intermediate times. At late times, the experimental data exhibit a crossover to a different scaling behavior. We attribute this to the problem becoming effectively three dimensional due to accumulation of particles at the shock front, and propose a simple hard sphere model which incorporates this effect. Simulations of this model capture the crossover seen in the experimental data.

PACS numbers: 45.70.-n, 45.70.Qj, 47.57.Gc

I. INTRODUCTION

Driven granular gases can produce complex and intricate spatial patterns [1–4]. Of particular interest is pattern formation following a localized perturbation, the subject matter of many recent experiments. Examples include crater formation by wind jets in the context of lunar cratering [5], viscous fingering in grains confined in a Hele-Shaw cell when displaced by gas or liquid [6–8], shock propagation in flowing glass beads following a sudden impact [9], signal propagation in dilute granular gas [10] as well as in dense static granular material (see [11] and references within), and avalanches in sand piles [12].

In this paper, we focus on an experiment [9] (henceforth referred to as BCK) on a dilute monolayer of glass beads flowing on an inclined glass plane. In the experiment, a steel ball, much larger in size than an individual glass bead, is dropped from a height onto the flowing beads. The impact generates a circular region, devoid of glass beads, whose radius increases with time. This radius was measured using high speed cameras. A theoretical model was proposed, and analyzed to derive an equation obeyed by the radius, whose solution predicts a logarithmic growth at large times. The numerical solution of the equation was shown to match with the experimental data [9].

In an independent study, we had studied the effect of exciting a single particle in a system of stationary hard inelastic particles using event driven molecular dynamics simulations, and scaling arguments [13]. By identifying radial momentum as a conserved quantity, and using scaling arguments, the radius of disturbance was predicted to

increase with time as a power law $t^{1/3}$ in two dimensions. This result was shown to be in very good agreement with data from numerical simulations of the model.

The inelastic hard sphere model closely resembles the experimental system in BCK, in the limit when the impact is very intense. In this paper, we propose the power law $t^{1/3}$ as an alternate description of the radius of disturbance in the BCK experiment. By reexamining the data in BCK, we show that, there are temporal regimes in which the power law growth is a good description. At late times, the experimental data deviate from the $t^{1/3}$ behavior. This, we argue is due to the experimental system becoming effectively three dimensional, and propose a simple model incorporating this effect. Our numerical data, obtained from simulations of this model, show clearly the crossover and captures the long time behavior. Since these results are in contradiction to those presented in BCK, we further analyze the model proposed in BCK, and point out some shortcomings. In particular, we show numerically that the main assumption of BCK is not correct. Though the experimental data are not able to distinguish between the two theories because the time scales are not large enough, the simulation data clearly bring out the deficiencies of the BCK theory at large times.

The experiment in BCK is the inelastic version of the classic Taylor-von Neumann-Sedov problem of shock propagation following a localized intense explosion [14]. In the latter case, the exponents characterizing the power law growth of the radius of the disturbance follows from energy conservation and simple dimensional analysis [15], while the scaling functions can be calculated exactly following a more detailed analysis [14, 16]. Theoretical, numerical and experimental studies of this problem are summarized in Refs. [17, 18]. Simulations in a hard sphere model with elastic collisions reproduce the results based on scaling arguments [19].

The BCK experiment is also a special case of a freely cooling gas (in a reference frame moving with mean veloc-

*Electronic address: sudhirnp@imsc.res.in

†Electronic address: zjabeen@umich.edu

‡Electronic address: ray@imsc.res.in

§Electronic address: rrajesh@imsc.res.in

ity of particles) wherein, after the initial input of energy, the system is isolated and allowed to freely evolve without any external driving. A key feature of the freely cooling granular gas is the clustering due to inelastic collisions. The freely cooling gas is well understood in one dimension and progressively less understood as the dimension increases [20–35]. Such systems are challenging experimentally because inelasticity is overwhelmed by friction and boundary effects. Friction can be eliminated in experiments on particles under levitation [36] or in microgravity [37, 38], but are expensive to perform and are limited by small number of particles and short times. In BCK, friction is balanced by gravity, and at high enough impact energies, in the center of mass frame, mimics a stationary collection of inelastic particles without friction. The boundary effects are eliminated as long as the shock does not reach the edges of the container. Thus, it is an experiment where clustering due to inelastic collisions can be studied easily.

The rest of the paper is organized as follows. In Sec. II, we describe the theoretical model in BCK, and review the arguments that lead to the equation obeyed by the radius of the disturbance. This equation is further analyzed to derive the asymptotic long time behavior. The shortcomings of this model are pointed out. We then, in Sec. III define a hard core inelastic gas model on which our computer simulations are performed. In Sec. IV, we demonstrate that our model reproduces the basic features of the experiment in BCK. The assumptions of the analysis in BCK is tested within this model and counter evidence is presented. In Sec. V, we compare the experimental results in Ref. [9] with the power law growth rules obtained in Ref. [13]. The data at intermediate times are well described by these power laws. However, there is a crossover to a different behavior at large times. In Sec. VI, we examine whether this large time behavior can be explained in terms of velocity fluctuations of the particles or by making the rim three dimensional. We argue that it is plausible that the three dimensional rim is responsible for deviation from power law growth and verify this by simulation. The results are summarized in Sec. VII.

II. BCK MODEL AND ANALYSIS

We first review the model studied in BCK to explain the experimental data. The model is based on the experimental observation, that after the impact with the steel ball, the displaced glass beads form a growing circular ring, devoid of beads. BCK considered an idealized model where all the particles contained in a disk of radius $R(t)$ at time t accumulate at the rim (boundary of ring). The remaining particles that are outside the disk are assumed to be stationary. This mimics the experimental system when one transforms to the center of mass coordinates, and in the limit of large impact energy, when the fluctuations of the particle velocities about the mean

flow may be ignored. Each particle at the rim is assumed to move radially outwards with a speed $V(t)$. As the ring moves outwards, more particles are absorbed into the ring. We reproduce the calculation in BCK, but generalized to d -dimensions. The total kinetic energy $E(t)$ is

$$E(t) = \frac{1}{2} \rho_0 \Omega_d R(t)^d V(t)^2, \quad (1)$$

where ρ_0 is the initial mass density, and Ω_d is the volume of a unit sphere in d -dimensions, such that $\rho_0 \Omega_d R(t)^d$ is the total mass of displaced particles. The speed $V(t)$ is

$$V(t) = \frac{dR(t)}{dt}. \quad (2)$$

One more relation between $E(t)$ and $R(t)$ is required for the solution. If the particles were elastic, then total energy is conserved, $E(t) \sim t^0$, and one obtains $R(t) \propto t^{2/(d+2)}$; in particular, $R(t) \propto \sqrt{t}$ in $d = 2$ [15]. However, when particles are inelastic, there is no such conservation law, and energy decreases with time. BCK proceed by the following argument. If r is the coefficient of restitution, then the loss of energy when a particle in the rim collides with a stationary particle outside is $\frac{1}{2}(1 - r^2)V(t)^2$. Thus, when the ring moves out by a distance dR , then the change in energy dE is given by

$$dE = -\frac{1}{2} \Omega R(t)^d \rho_0 V(t)^2 (1 - r^2) N(t) dR, \quad (3)$$

where $N(t)$ is the number of collisions per particle per unit length, or equivalently, $N(t)dR$ is the number of collisions for each particle in the rim as it travels a distance dR . BCK makes the strong assumption that $N(t)$ is independent of the radius, and hence time t that is,

$$N(t) = \text{constant}. \quad (4)$$

Eliminating $R(t)$ and $V(t)$ in Eq. (3) using Eq. (1), one obtains

$$E(t) = E_0 \exp[-N(1 - r^2)R(t)], \quad (5)$$

where E_0 is the energy of impact at $t = 0$. It is now straightforward to obtain the equation satisfied by the radius $R(t)$:

$$\frac{t}{t_0} = \int_0^{R/R_0} dx x^{d/2} e^x, \quad (6)$$

where $t_0^{-1} = \sqrt{E_0 [N(1 - r^2)]^{d+2} / (\rho_0 \Omega_d 2^{d+1})}$ and $R_0^{-1} = N(1 - r^2)/2$.

For later reference, it will be useful to derive the asymptotic solutions to Eq. (6). Let $\alpha = \ln(t/t_0)$. Then for large times, it is straightforward to derive:

$$\frac{R}{R_0} = \alpha \left[1 - \frac{d \ln \alpha}{2 \alpha} + \frac{d \ln \alpha}{2 \alpha^2} + O\left(\frac{1}{\alpha^2}\right) \right], \quad \alpha \gg 1. \quad (7)$$

The growth is logarithmic at large times in all dimensions. For short times, by writing the exponential in Eq. (6) as a series, it is easy to obtain

$$\frac{R}{R_0} = \left[\frac{(d+2)t}{2t_0} \right]^{\frac{2}{d+2}} \left[1 + O\left(\left(\frac{t}{t_0} \right)^{\frac{2}{d+2}} \right) \right], t \ll t_0. \quad (8)$$

For small times, the power law growth of radius is identical to the elastic case [15].

The experimental data in BCK was fitted to the numerical solution of Eq. (6) with $d = 2$. Although the equation describes the data well (see Fig. 4 of Ref. [9]), we now argue that the analysis has certain shortcomings, making the results questionable.

First, we show by a simple calculation that the solutions Eqs. (5) and (6) do not give the correct results when $d = 1$. The solution Eqs. (5) and (6) are valid for all values of $r < 1$, including $r = 0$. In one dimension, the special case $r = 0$, when particles stick on collision, is easily solvable [13]. Let particles of mass m be initially placed equidistant from each other with inter-particle spacing a . Pick a particle at random and give it a velocity v_0 to the right. When this particle collides with its neighbor, it coalesces with it. After k collisions, the mass of the composite particle is $(k+1)m$, its distance from the impulse is $R = ka$, and its velocity, given by momentum conservation, is $v_k = v_0/(k+1)$ towards the right. The time taken for k collisions is given by

$$t_k = \sum_{i=0}^{k-1} \frac{a}{v_i} = \frac{ak(k+1)}{2v_0}. \quad (9)$$

Solving for k , we obtain $k = (-1 + \sqrt{1 + 8tv_0/a})/2$. At large times $t \gg a/v_0$, the radius and energy are $R = ka \approx \sqrt{2v_0at}$ and $E(t) = mv_0^2a/(2R)$. The analysis in BCK for energy [Eq. (5)] and radius $R(t)$ [Eq. (7)] are not consistent with the exact solution in one dimension.

Second, we show that the long time logarithmic growth of the radius of the disturbance, as in Eq. (7), is not possible. We note that the radial momentum in a fixed direction cannot decrease. It can decrease only if the pressure outside the growing circular ring is larger than the pressure inside. However, the outside pressure is zero since all the particles are stationary, and the inside pressure is non-negative since it is a collection of hard-core repulsive particles. Thus, the radial momentum of the system cannot decrease with time. Suppose we assume that Eq. (7) is right, ie, $R(t) \sim \ln t$. In two dimensions, the radial momentum is $R(t)^2V(t)$, where $V(t) = dR/dt \sim 1/t$. Thus the radial momentum scales as $(\ln t)^2/t$, implying that the radial momentum decreases with time, which is impossible. Therefore, within the model, the logarithmic time dependence of the radius is not possible. The above argument that the radial momentum cannot decrease with time puts bounds on the growth exponent of the radius of disturbance. Assume that $R(t) \sim t^\alpha$, $t \gg 1$. Then, radial momentum scales as $t^{3\alpha-1}$. We immediately obtain that the radius cannot grow more slowly than $R \sim t^{1/3}$, within the framework of the model.

We now argue that radial momentum is not just non-decreasing, but a constant of motion. Every collision is momentum conserving. In addition, the clustering of all the displaced particles at the rim of the ring prevents momentum being transferred in the negative radial direction. If we further assume that once the dense rim is formed, the angular coordinates of particles do not change much, then radial momentum is a constant of motion (see also discussion on Fig. 2 in Sec. IV). Therefore,

$$\Omega_d R(t)^d V(t) \Delta\theta = \text{constant}, \quad (10)$$

where $\Delta\theta$ is the angular spread in direction θ . The solution to Eq. (10) is

$$R(t) \propto t^\alpha, \quad t \gg t', \quad (11)$$

where $\alpha = 1/(d+1)$, and t' is the initial mean collision time. Equivalently $R(t)^{d/2} \sqrt{E(t)}$ is a constant of motion. Equation (5) is clearly not consistent with this constraint, neither is Eq. (7) for growth of radius consistent with Eq. (11).

We, therefore, conclude that the analysis of BCK is not completely satisfactory. Since the solution of BCK [Eqs. (5) and (6)] was based on the assumption that $N(t)$, the rate of collisions per particle per unit distance, is a constant, we test the validity of this assumption as well as the prediction of Eq. (6) in molecular dynamics simulations of a hard sphere gas. As we will argue below, the theory presented in BCK is also applicable to the hard sphere model.

III. MODEL FOR SIMULATION

The system which is simulated is defined as follows. Consider a collection of identical particles, modeled as hard spheres, in two dimensions. The mass and diameter of the particles are set to unity. All the particles are initially at rest and have a packing density 0.20, much smaller than the known random closed packed density 0.84 in two dimensions [39, 40]. We model an isotropic impulse by introducing four particles at the center with speed v_0 in the directions $0, \pi/2, \pi$, and $3\pi/2$. Particles interact only on collision, during which momentum is conserved and velocities change deterministically. If the velocities of two particles 1 and 2 before and after collision are $\mathbf{u}_1, \mathbf{u}_2$, and $\mathbf{v}_1, \mathbf{v}_2$ respectively, then

$$\mathbf{v}_{1,2} = \mathbf{u}_{1,2} - \epsilon [\mathbf{n} \cdot (\mathbf{u}_{1,2} - \mathbf{u}_{2,1})] \mathbf{n}, \quad (12)$$

where $r = 2\epsilon - 1$, ($0 < r < 1$) is the coefficient of restitution and \mathbf{n} is the unit vector directed from center of particle 1 to the center of particle 2. In words, the tangential component of the relative velocity remains unchanged, while the magnitude of the longitudinal component is reduced by a factor r . When $r = 1$, the collisions are elastic. To simulate the inelastic system, the

coefficient of restitution r is chosen to be less than unity if the magnitude of the longitudinal component of the relative velocity is greater than a velocity scale δ , else $r = 1$ mimicking elastic collisions for small relative velocities [26]. This qualitatively captures the experimental situation where r is seen to be a function of the relative velocity [41, 42]. In addition, it prevents inelastic collapse that is a hindrance to simulations [43, 44]. The cutoff δ introduces a timescale in the problem at large times, after which most of the collisions are elastic. For sufficiently small δ , the elastic crossover timescale does not show up in our simulations.

We simulate the system in two dimensions using event driven molecular dynamics [45]. The data presented are typically averaged over 8 different initial realizations of the particle configurations. All lengths are measured in units of the particle diameter, and time in units of initial mean collision time $t_0 = v_0^{-1}n^{-1/d}$, where v_0 is the initial speed and n is the number density. The value of δ is 10^{-4} , unless specified otherwise. For these values of δ , all the quantities that we measure except for the rate of collisions are independent of δ [13]. The initial speed is $v_0 = 1$ unless specified otherwise.

IV. NUMERICAL STUDY OF BCK RESULTS

In this section, the results and assumption of BCK are checked in numerical simulation of the hard sphere model. In Fig. 1, we show the time evolution of the system following an impulse. As time increases, all the particles that were originally in a roughly circular ring, cluster together at its rim. We observe clustering for all the values of $r < 1$ that we have simulated, with clustering setting in at later times for larger coefficients of restitution.

The formation of an empty region bounded by the moving particles (as in Fig. 1) is the only requirement for the BCK theory to be applicable. Therefore, if the analysis in BCK is correct, then the results for radius in Eq. (6) should describe the disturbance in the hard sphere model too. In numerical simulations, data can be obtained for much longer times than that in the experimental data in Ref. [9], and therefore be used to make a more rigorous test of the assumptions and the conclusions of the BCK theory.

We first present numerical evidence for radial momentum being a constant of motion, as argued in Sec. II. In Fig. 2, the temporal variation of the radial momentum is shown for different δ with fixed $r = 0.10$ and compared with the data for the elastic problem. When all collisions are elastic, radial momentum increases as \sqrt{t} . When collisions are inelastic, radial momentum increases very slowly with time from an initial value of 4.0 to 8.6, in nearly six decades of time (see inset of Fig. 2). With the current data, it is not possible to conclude with certainty that radial momentum will become a constant at large time when $\delta \rightarrow 0$. However, one can rule out a

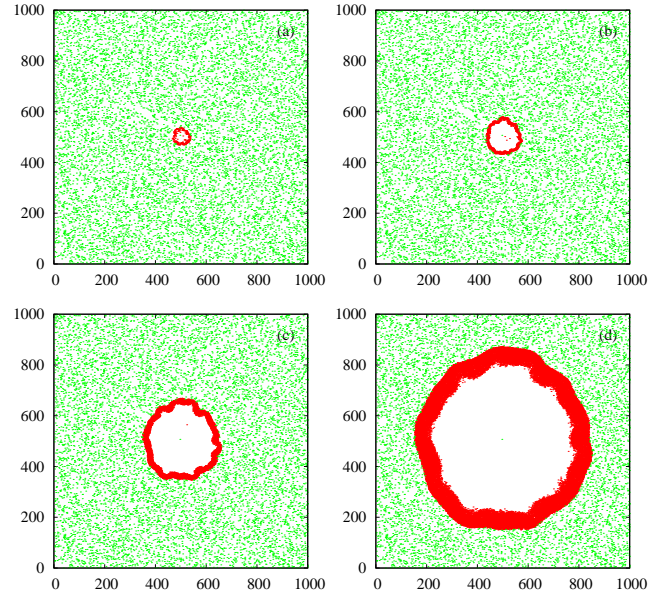


FIG. 1: (Color online) Moving (red) and stationary (green) particles at times $t =$ (a) 10^3 , (b) 10^4 , (c) 10^5 and (d) 10^6 , following an isotropic impulse at $(500, 500)$ at $t = 0$. The moving particles cluster together at the disturbance front. The data are for $r = 0.10$.

power law growth. The radial momentum conservation is strictly valid only when collisions are completely inelastic, $r = 0$ and $\delta = 0$. However, for other value of r and δ , even after formation of the circular band, colliding particles may change their angular coordinates. Such changes in the angular coordinates of the particles will result in increase of radial momentum. We checked that the average change in angle following a collision decreases to zero with time.

In Fig. 3, we compare the BCK result Eq. (6) for the radius with hard sphere simulation data. The constants R_0 and t_0 in Eq. (6) are determined by fitting it to the numerical data at early times. It is clear that Eq. (6) captures only the short time behavior. On the other hand, the data at large times are consistent with the power law $t^{1/3}$. We believe that the discrepancies between the short and large time behavior are not brought out by the experimental data as the time scales are not large enough.

We now make a direct test of the BCK assumption that $N(t)$, the number of collisions per particle per unit distance is a constant in time, as assumed in BCK. The data for $N(t)$ are shown in Fig. 4 for three different coefficients of restitution, one of them being $r = 1$. While $N(t)$ is a constant when collisions are elastic, it is clearly not so for $r < 1$, invalidating the BCK assumption. At large times, the rate of collisions become independent of r as long as $r < 1$. This is consistent with the observations in the freely cooling granular gas [26, 27], where the long time behavior of $E(t)$ and $N(t)$ is independent of r , and hence identical to $r = 0$, the sticky limit. Thus we

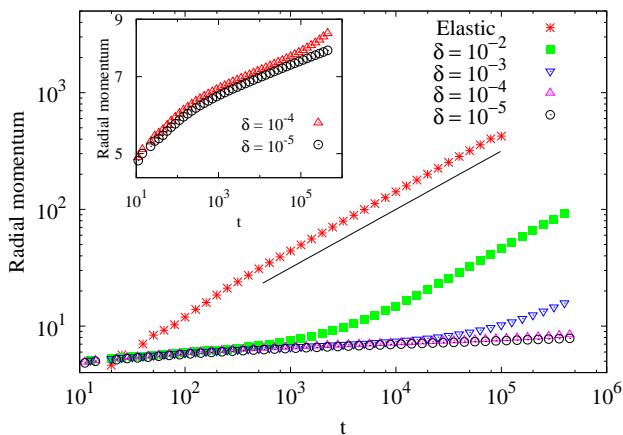


FIG. 2: (Color online) The radial momentum as a function of time t . For elastic collisions, it increases as \sqrt{t} (the solid straight line is a power law \sqrt{t}). For inelastic collisions with $r = 0.10$, the radial momentum appears to increase very slowly with time to a constant, when $\delta \rightarrow 0$. The slow increase of the radial momentum can be seen more clearly in the inset. The data for the elastic system have been scaled down by factor $1/2$.

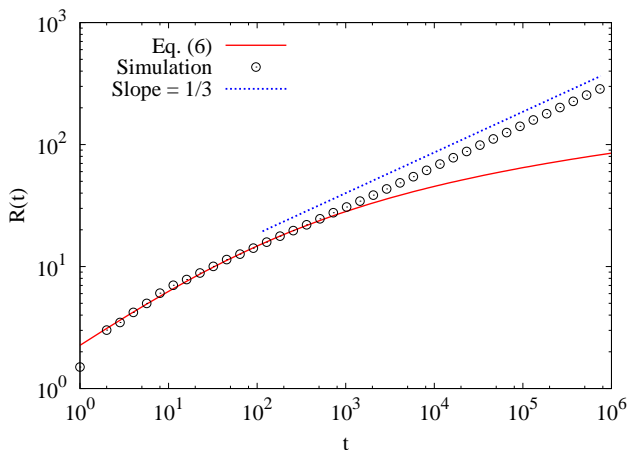


FIG. 3: (Color online) Data for radius $R(t)$ from simulations in two dimensions are compared with Eq. (6) and $t^{1/3}$. R_0 and t_0 in Eq. (6) are obtained by fitting the initial time simulation data to Eq. (6) and are $R_0 = 10.30 \pm 0.21$ and $t_0 = 35.79 \pm 2.35$. The data are for $r = 0.10$.

could think of the rim as a solid annulus made up of all the particles that have undergone at least one collision. Therefore, once the rim forms, we expect that only the collisions of the particles that are at the outer edge of the rim, with the stationary particles are relevant. Then, the collisions per particle on surface per unit time, NR , should be constant. This is confirmed in the inset of Fig. 4, where NR tends to a constant independent of r , at large times. Since the relevant collisions are taking place at the outer boundary of the rim, Eqs. (5) and (6) underestimate the radius, or equivalently overestimate

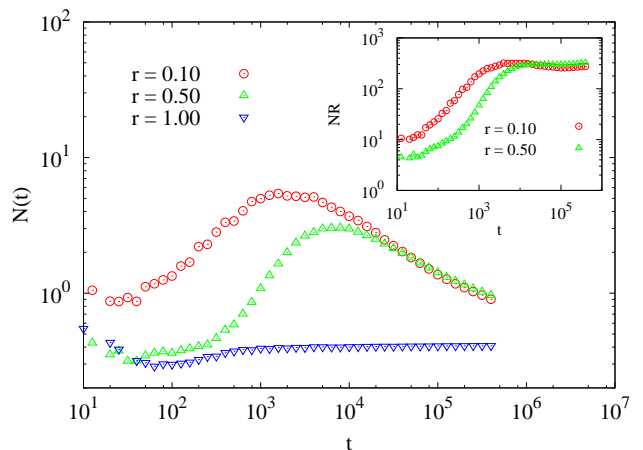


FIG. 4: (Color online) Temporal variation of $N(t)$, the number of collisions per particle per unit distance for various r . For $r < 1$, $N(t)$ is not constant as assumed by BCK. Inset: NR , where R is the radius of disturbance, is a constant at large times for $r < 1$.

energy loss.

V. COMPARISON WITH EXPERIMENTAL DATA

In this section, we compare the power law solution $R(t) \sim t^{1/3}$, obtained from the conservation of radial momentum, with the experimental data of Ref. [9]. Figure 5 shows the data (Fig. 4 of Ref. [9]) for the temporal variation of the radius of disturbance $R(t)$ following impacts with spheres of different diameter. The black solid lines are power laws $t^{1/3}$. There are temporal regimes where it matches well with the experimental data. However, there are deviations from $t^{1/3}$ at large times. There is sufficient statistics for this late time regime only for the impact with the largest sphere. For this data, we find that the data are best fitted by a power law $t^{0.18}$ (see dashed line in Fig. 5).

The experimental situation is more complicated than the simple hard sphere model for which the power law growth is presumably the correct result. To equate the two, we had to make approximations. First, we ignored the fluctuations of the velocities of the particles about the mean velocity. While this is reasonable for large impact velocities when typical speeds of displaced particles are much larger than typical velocity fluctuations, the fluctuations become relevant at late time. Second, we ignored the experimentally observed three dimensional nature of the rim (see discussion in last but one paragraph of Ref. [9]). Such a possibility will result in radial momentum not being conserved, thus invalidating the scaling arguments in [13].

It is possible that either or both of these approximations could be responsible for the crossover seen at large times. In Sec. VI, we study modified versions of the hard

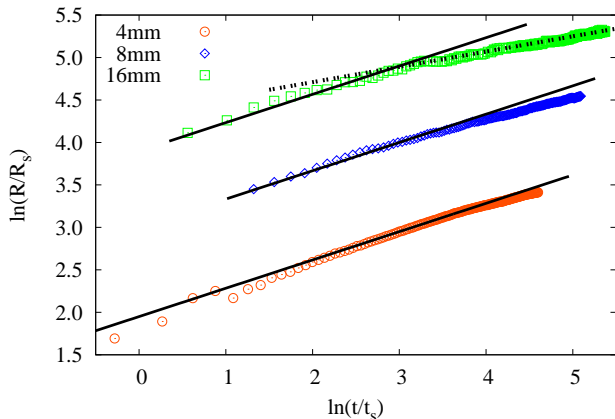


FIG. 5: (Color online) Experimental data from Ref. [9] for radius R as a function of time t following an impact by steel balls of diameter 4 mm, 8 mm and 16 mm. The solid/dashed lines have slope $1/3$ and 0.18 respectively. R_s is the diameter of a glass bead and t_s is the mean time taken by a glass bead to traverse a distance equal to its diameter. The data have been obtained from Ref. [9].

sphere model, which incorporates the above features. We argue that the crossover from $t^{1/3}$ law can be explained by these models.

VI. EFFECT OF NON-ZERO AMBIENT TEMPERATURE AND THREE DIMENSIONAL RIM

In the center of mass coordinates, all particles are not stationary but fluctuating about their mean position. When these velocity fluctuations become comparable to the velocity of the rim, then we expect the rim to destabilize, and power laws to show crossovers.

We model this situation as follows. Initially all the particles (type E) are assumed to be elastic and equilibrated at a certain fixed temperature, parameterized by $\Lambda^2 = \langle v^2 \rangle / v_0^2$, where $\langle v^2 \rangle$ is the mean velocity fluctuations and v_0 , as earlier, is the speed of the perturbed particles. $\Lambda = 0$ corresponds to the case when all particles are initially stationary. An isotropic impulse is imparted by introducing four particles (type I) at the center with speed v_0 in the directions $0, \pi/2, \pi,$ and $3\pi/2$. Collisions between E particles are elastic. Collisions involving at least one I particle are inelastic. If an E particle collides with an I particle, then it becomes type I . This model captures shock propagation in a system where all particles have some nonzero kinetic energy.

In Fig. 6, we show snapshots of the system at various times, when the $\Lambda = 1/800$. The sharp rim starts becoming more diffuse as the velocity of the rim decreases, until the enclosed empty region vanishes completely. These snapshots are qualitatively very similar to that seen in the experiment for low speed impacts and at large times

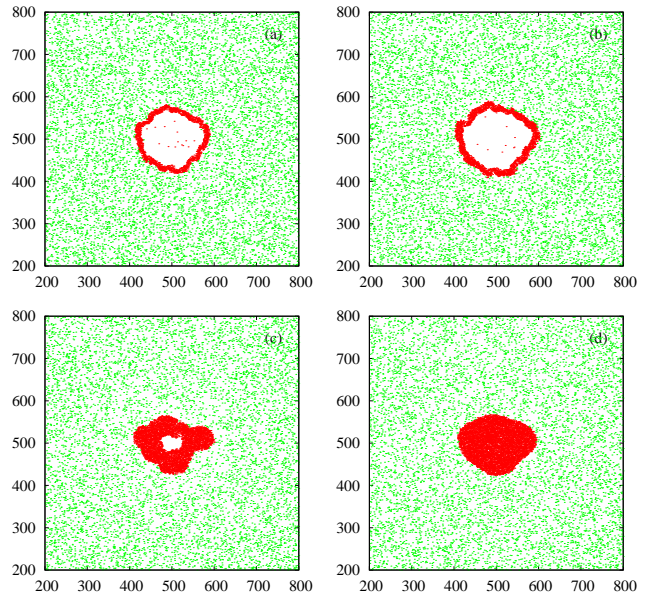


FIG. 6: (Color online) Snapshots of inelastic I particles (red) and elastic E particles (green), when $\Lambda = 1/800$, following an isotropic impulse at $(500, 500)$ at $t = 0$. The time increases from (a) to (d) and correspond to the times shown by labels a–d in Fig. 7. Initially, the disturbance grows as in Fig. 1, but at late times due to velocity fluctuations, the rim gets destabilized. The data are for $r = 0.10$.

(see Fig. 1 of Ref. [9]).

When the rim destabilizes, $R(t)$ shows deviation from the $t^{1/3}$ power law growth (see Fig. 7). It is straightforward to estimate this crossover time t_c . The instability sets in when the speed of the rim is of the same magnitude as the velocity fluctuations, i.e. $v_{t_c} \sim \Lambda v_0$. Since $v_t \sim dR/dt \sim t^{-2/3}$, we immediately obtain $t_c \sim \Lambda^{-3/2}$. Thus, $R(t)$ should have the scaling form

$$R(t) \sim t^{1/3} f\left(t\Lambda^{3/2}\right), \quad (13)$$

where $f(x)$ is a scaling function with $f(x) \sim O(1)$, when $x \rightarrow 0$. The curves for different Λ collapse when scaled as in Eq. (13) [see inset of Fig. 7].

The introduction of a finite ambient temperature, while leading to the disintegration of the rim, does not produce the large time behavior of the data for the radius. We now ask whether the rim becoming three dimensional could be responsible for that. The rim presumably becomes three dimensional because a fast particle when hemmed in by many surrounding particles may jump out of the plane due to collision with floor and friction. The net effect is a reduction in radial momentum, which could change the growth law.

To mimic radial momentum leakage occurring at high densities, we consider the following model. We divide the system into squares of length equal to diameter of the particles. Given the grid position of a particle, any particle which is in one of the eight neighboring squares

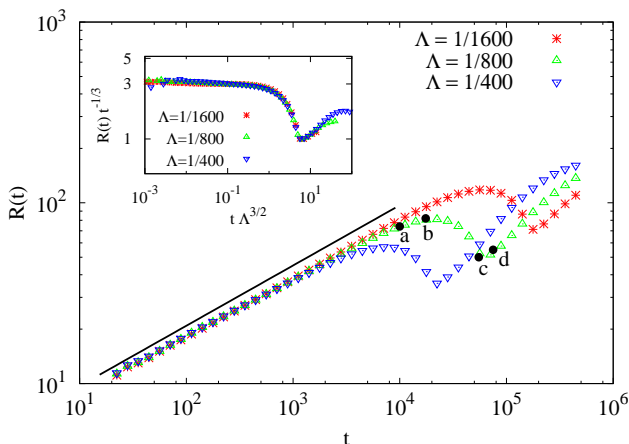


FIG. 7: (Color online) The radius of disturbance $R(t)$ as a function of time t for different values of Λ . The effect of velocity fluctuations are felt later for smaller Λ . At large times, the finite external pressure is able to compress the bubble, with $R(t)$ reaching a minimum when the density of the bubble approaches the close packing density. Inset: Data collapse when scaled according to Eq. (13). A solid line of slope $1/3$ is drawn for reference. The data are for $r = 0.10$.

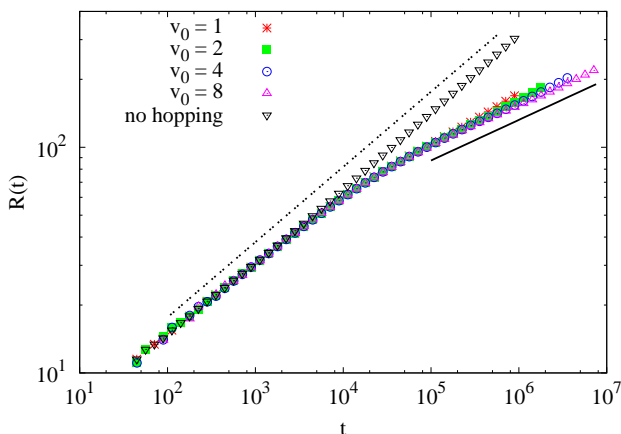


FIG. 8: (Color online) Temporal variation of radius $R(t)$ for $\kappa = 0.20$ with various initial velocity v_0 . The solid line is a power law $t^{0.18}$ while the dashed line is a power law $t^{1/3}$. The data with no hopping correspond to $v_0 = 1$. All data are for $r = 0.10$.

will be called its neighbor. At any instant of time, if a particle has eight or more neighbors, then we remove the particle if its velocity \mathbf{v} satisfies the hopping criterion, $(\mathbf{v} - \mathbf{v}_{cm}) \cdot \hat{\mathbf{v}}_{cm} > \kappa v_{cm}$, where \mathbf{v}_{cm} is the center of mass velocity of the particle and its neighbors. In words, the longitudinal component of the velocity should be larger than v_{cm} by a factor κ .

The hopping criterion is tested for all moving particles after every 100 collisions in the system, and the results do not depend on this number provided it is not too large. The results are shown in Fig. 8. The results obtained

are insensitive to the value of κ provided $\kappa < 0.20$. We find that at large times, the system crosses over to a different power law growth $\approx t^{0.18}$, that is very similar to the growth law seen in the experiment. While the aim of the model was to show that loss of radial momentum, at high densities, can result in crossovers at large times, we obtain a quantitative match. As of now, we have no explanation why the exponents have approximately the same numerical value, and it could be just a coincidence.

VII. CONCLUSION AND DISCUSSION

In summary, we analyzed the recent experiment [9] of dropping spheres onto a flowing monolayer of glass beads. We modeled the experiment with a hard sphere system undergoing inelastic collisions. With this hard sphere system, we showed that the assumption of constant rate of collision per particle per unit distance, made in the theory [9] to describe the experimental data is correct only for elastic particles. For inelastic system, the relevant collisions are the collisions of the particles at the outer edge of the rim with the stationary particles outside. We also argued that the formation of the circular ring in the perturbed system conserves radial momentum. This conservation law leads to a $t^{1/3}$ power law growth for the radius of disturbance. The $t^{1/3}$ growth law describes the experimental data well except at large times when the data show a crossover to a different power law growth. We attributed this crossover to the rim becoming three dimensional because of high densities and collisions with the floor. By constructing a simple model incorporating these effects, we were able to explain the crossovers at large times.

The current experimental data can not distinguish between the theory in BCK and the power law growth argued for in this paper. If the experimental time scale is increased, then such a distinction may be possible. It will be worthwhile to make the attempt.

In our simulations, we modeled the coefficient of restitution as $r < 1$ for relative velocities larger than a velocity scale δ and $r = 1$ otherwise. The velocity scale δ is relevant experimentally and not just a computational tool. Experimentally, $r(v)$ approaches 1 when the relative velocity v tends to zero, i.e., $1 - r(v) = g(v/\delta)$, where $g(x) \sim x^\chi + O(x^{2\chi})$, for $x \ll 1$ and $g(x) \sim O(1)$ for $x \rightarrow \infty$, and the exponent χ takes a variety of values. Within the framework of viscoelastic theory, $\chi = 1/5$ [46]. Systems with $\chi < 1$ cannot be studied using the event driven molecular dynamics simulations performed in this paper, as inelastic collapse prevents the simulation from proceeding forward. However, we have checked, using molecular dynamics simulations with soft potentials, that the rim formation and radius increasing as a power law $t^{1/3}$ continue to be true for $\chi < 1$ [47].

It will be quite interesting to see if any connection can be made between the shock problem in which most of the particles are initially stationary and the well studied

freely cooling granular gas, in which all particles initially have a nonzero kinetic energy. It may be possible to think of the freely cooling gas as a collection of shocks initiated at different points in space, which interact when the shock fronts meet. If such a connection is possible, it will help in resolving the uncertainty of the energy decay exponent [21, 27] of the freely cooling granular gas. Thus, it will be useful to make a detailed study of the case of two interacting shocks.

The data for radius show a crossover from an initial elastic behavior $t^{1/2}$ to an asymptotic $t^{1/3}$ growth law. It would be of interest to understand this crossover better. Exact solution of the shock problem in one dimension with $0 < r < 1$ would throw light on it. An exact solution appears possible given that the freely cooling in one di-

mension is one of the exactly solvable model in granular physics.

Acknowledgments

We thank the authors of Ref. [9] for providing us with the experimental data. We thank an anonymous referee for providing the argument that radial momentum cannot decrease in an expanding hard-core gas. All simulations were carried out on the Intel Nehalem 2.93 GHz supercomputing machine Annapurna at The Institute of Mathematical Sciences.

-
- [1] H. M. Jaeger, S. R. Nagel, and R. P. Behringer, *Rev. Mod. Phys.* **68**, 1259 (1996).
 - [2] L. P. Kadanoff, *Rev. Mod. Phys.* **71**, 435 (1999).
 - [3] A. Kudrolli, *Rep. Prog. Phys.* **67**, 209 (2004).
 - [4] I. S. Aranson and L. S. Tsimring, *Rev. Mod. Phys.* **78**, 641 (2006).
 - [5] P. T. Metzger, C. D. Immer, C. M. Donahue, B. M. Vu, R. C. L. III, and M. Deyo-Svendsen, *J. Aerospace Engineering* **21**, 24 (2009).
 - [6] X. Cheng, L. Xu, A. Patterson, H. M. Jaeger, and S. R. Nagel, *Nat. Phys.* **4**, 234 (2008).
 - [7] B. Sandnes, H. A. Knudsen, K. J. Måløy, and E. G. Flekkøy, *Phys. Rev. Lett.* **99**, 038001 (2007).
 - [8] S. F. Pinto, M. S. Couto, A. P. F. Atman, S. G. Alves, A. T. Bernardes, H. F. V. de Resende, and E. C. Souza, *Phys. Rev. Lett.* **99**, 068001 (2007).
 - [9] J. F. Boudet, J. Cassagne, and H. Kellay, *Phys. Rev. Lett.* **103**, 224501 (2009).
 - [10] W. Losert, D. G. W. Cooper, and J. P. Gollub, *Phys. Rev. E* **59**, 5855 (1999).
 - [11] S. Luding, *Nature* **435**, 159 (2005).
 - [12] A. Daerr and S. Douady, *Nature* **399**, 241 (1999).
 - [13] Z. Jabeen, R. Rajesh, and P. Ray, *Eur. Phys. Lett.* **89**, 34001 (2010).
 - [14] L. Sedov, *Similarity and Dimensional Methods in Mechanics* (CRC Press, Florida, 1993), 10th ed.
 - [15] G. Taylor, *Proc. R. Soc. Lond. A* **201**, 159 (1950).
 - [16] J. von Neumann, in *Collected Works* (Pergamon Press, Oxford, 1963), p. 219.
 - [17] Y. B. Zel'dovich and Y. P. Raizer, *Physics of Shock Waves and High Temperature Hydrodynamic Phenomena* (Dover Publications, Inc., New York, 2002).
 - [18] J. P. Ostriker and C. F. McKee, *Rev. Mod. Phys.* **60**, 1 (1988).
 - [19] T. Antal, P. L. Krapivsky, and S. Redner, *Phys. Rev. E* **78**, 030301(R) (2008).
 - [20] P. Haff, *J. Fluid Mech.* **134**, 401 (1983).
 - [21] G. F. Carnevale, Y. Pomeau, and W. R. Young, *Phys. Rev. Lett.* **64**, 2913 (1990).
 - [22] R. Brito and M. H. Ernst, *Europhys. Lett.* **43**, 497 (1998).
 - [23] S. McNamara and W. R. Young, *Phys. Rev. E* **53**, 5089 (1996).
 - [24] E. Trizac and J.-P. Hansen, *Phys. Rev. Lett.* **74**, 4114 (1995).
 - [25] E. Trizac and A. Barrat, *Eur. Phys. J E* **3**, 291 (2000).
 - [26] E. Ben-Naim, S. Y. Chen, G. D. Doolen, and S. Redner, *Phys. Rev. Lett.* **83**, 4069 (1999).
 - [27] X. Nie, E. Ben-Naim, and S. Chen, *Phys. Rev. Lett.* **89**, 204301 (2002).
 - [28] S. Miller and S. Luding, *Phys. Rev. E* **69**, 031305 (2004).
 - [29] I. Goldhirsch and G. Zanetti, *Phys. Rev. Lett.* **70**, 1619 (1993).
 - [30] M. Shinde, D. Das, and R. Rajesh, *Phys. Rev. Lett.* **99**, 234505 (2007).
 - [31] M. Shinde, D. Das, and R. Rajesh, *Phys. Rev. E* **79**, 021303 (2009).
 - [32] S. Dey, D. Das, and R. Rajesh, *Eur. Phys. Lett.* **93**, 44001 (2011).
 - [33] S. Chen, Y. Deng, X. Nie, and Y. Tu, *Phys. Lett. A* **269**, 218 (2000).
 - [34] L. Frachebourg, *Phys. Rev. Lett.* **82**, 1502 (1999).
 - [35] E. Trizac and P. L. Krapivsky, *Phys. Rev. Lett.* **91**, 218302 (2003).
 - [36] C. C. Maaß, N. Isert, G. Maret, and C. M. Aegerter, *Phys. Rev. Lett.* **100**, 248001 (2008).
 - [37] S. Tatsumi, Y. Murayama, H. Hayakawa, and M. Sano, *J. Fluid. Mech.* **641**, 521 (2009).
 - [38] Y. Grasselli, G. Bossis, and G. Goutallier, *Euro. Phys. Lett.* **86**, 60007 (2009).
 - [39] D. E. G. Williams, *Phys. Rev. E* **57**, 7344 (1998).
 - [40] D. Bideau and J. P. Troadec, *J. Phys. C* **17**, L371 (1984).
 - [41] C. V. Raman, *Phys. Rev.* **12**, 442 (1918).
 - [42] E. Falcon, C. Laroche, S. Fauve, and C. Coste, *Euro. Phys. J. B* **3**, 45 (1998).
 - [43] S. McNamara and W. R. Young, *Phys. Fluids. A* **4**, 496 (1992).
 - [44] S. McNamara and W. R. Young, *Phys. Rev. E* **50**, R28 (1994).
 - [45] D. C. Rapaport, *The art of molecular dynamics simulations* (Cambridge University Press, Cambridge, 2004).
 - [46] N. V. Brilliantov and T. Pöschel, *Kinetic Theory of Granular Gases* (Oxford University Press, Oxford, 2004).
 - [47] S. N. Pathak, Z. Jabeen, R. Rajesh, and P. Ray, *Proceedings of the 56th DAE Solid State Physics Symposium (to appear)*.